Growth profile of *Chaetoceros* sp. and its steady state behaviour with change in initial inoculum size: a modelling approach

Sayani Kundu[1,3], Joyita Mukherjee[2], Farhana Yeasmin[1], Samarpita Basu[1,*], Joydev Chattopadhyay[1], Santanu Ray[3] and Sabyasachi Bhattacharya[1,]**

[1]Agricultural and Ecological Research Unit, Indian Statistical Institute, Kolkata 700 108, India
[2]Department of Zoology, Krishna Chandra College, Hetampur 731 124, India
[3]Systems Ecology & Ecological Modelling Laboratory, Department of Zoology, Visva-Bharati, Santiniketan 731 235, India

Monitoring and modelling of the growth profile of microalgae species should be an important tool for the hatchery industries before standardizing the best yielding and cost-effective protocol for their unit. Several factors are responsible in determining the nature of the growth profile. The most important regulator of such growth profile should be the volume of the initial inoculum. In addition, identification and determination of different phases (lag, log, stationary, etc.) of the growth curves of microalgae may be an essential part in the growth profile monitoring. Estimation of growth phases will also help the hatchery scientists in standardizing the commercial culture for industry. Moreover, the transition of different phases can be accurately identified through theoretical models, which are mostly overlooked in simple analysis. Summing up, we have two precise objectives: (1) to study the effects of choice of initial inocula levels on the time to maturity of the *Chaetoceros* sp., (2) to model the growth profile of the species from which we can theoretically determine its different phases, based on the optical density measurement as a proxy of the biomass. The estimated values of each phase are compared under two initial inocula levels through statistical tests. Using the conceptual approach of the proposed theoretical technique, there is scope for developing a similar model, which can be used in determining cost-effective culture protocol for commercial use.

Keywords: Cost-effective production, growth profile, hatchery industry, initial inoculum, optical density.

MICROALGAE are used as exclusive live food for commercially valuable fish and shellfish in hatchery. Microalgae play a crucial role in aquaculture as it provides protein (essential amino acids) along with other key nutrients and vitamins, essential PUFAs, pigments and sterols. As a consequence, the fish community or the zooplankton species may be directly or indirectly benefited[1].

Among many microalgae identified for aquaculture purposes, species belonging to the genera, *Chaetoceros* and *Isochrysis* are extensively used as food in most of the shrimp hatcheries[2]. However, *Chaetoceros* is generally preferred over *Isochrysis* because of its ability for rapid growth and its nutritional superiority, particularly owing to higher content of unsaturated fatty acids[3]. Hence, *Chaetoceros* sp. is chosen as the sample organism for the present investigation on growth profile study with variation in the initial inoculum volume. Microalgal culture is the most expensive and technically challenging aspect of all the hatchery operations[4]. There are several lacunae involved during the production and screening practices of microalgae in the hatcheries[5]. Some of these problems are associated in maintaining overall sterility of culture ingredients, continuous supply of artificial light and oxygen, temperature control, advanced instruments like Coulter counter, digital microscopy, etc.[6]. The inconvenience involved in such maintenance could appear at different stages of the growth process. The exact change point of different phases of the growth profile could identify these stages more precisely with the help of theoretical models. The experimenter can take advantage from this theoretical model in tuning maintenance parameters for optimum culture. Optimum culture condition can be defined as the ideal condition, which is the most favourable environment for maximum growth of the microorganism[6]. Optimization can be achieved by trading off the production cost and profit by tuning maintenance parameters and theoretical models. The researchers, working in this domain should search for a less-complex (easy) culture technique in terms of maintenance parameters, commercially successful, cost-effective (cheap) production and finally a consistent (reliable) culture technique with minimum experimental errors[7].

Algal cells from a starter culture are inoculated into a larger volume of treated, enriched water to reach an optimal level from the initial low density. The optimum

*A part of laboratory experiment is done during her visit at Indian Statistical Institute, Kolkata.

**For correspondence. (e-mail: sabyasachi@isical.ac.in)

culture technique is heavily dependent on the amount of inoculum used at the initial stage of experiment[4]. Some additional physical factors such as temperature, light intensities, amount of CO_2, etc., are also important for phytoplankton growth[8,9]. *Chaetoceros* sp. do not accumulate internal pools of inorganic nutrients whose uptake and growth of the individual are closely coupled; therefore, it processes the nutrient pulses very rapidly into the new cells[10]. As a result, the lag phase may be shorter for this species (table 3 of ref. 10). At the low inoculum level, the population density of the species is less and as a consequence the nutrient uptake is low. The scenario is just reverse if we have a higher concentration of inoculum. So the chance of unutilized nutrient at the steady state is higher for the first case compared to the second[11]. In addition, a comparative growth study with equal volume of initial inoculum of mixed and mono cultures of *Isochrysis galbana* and *Chaetoceros calcitrans* was considered to observe the symbiotic nature of those species, although the experiments with different initial inocula levels were ignored here[12]. There may be a possibility that the variation with the inoculum level at initial stage of the growth experiment may change the span of the lag, log phases which lead to the change in the growth profile of the species.

Thus, in this study we have two-fold objectives: (1) to study the relationship between the choice of initial inocula levels and the time to maturity of *Chaetoceros* sp. (economically an important microalga), (2) to model the complete growth profile of species, so that we can theoretically determine and compare the deviation of lag, log, stationary and decay phases of the species with different inocula levels. It is expected that, the individuals present at low inoculum density are exposed to less competition compared to those present at high inoculum density, if both the populations are kept in the same medium with equal amount of nutrients. Variation in competition level due to change in inoculum level would result in deviation from the growth trajectory under fixed nutrient environment. Discrepancy in competition and its relationship with abundance through reproduction is generally complex in nature. Modelling growth trajectories under different competition levels can be a good alternative for understanding this relationship. The modelling based on the relationship can help the experimental and hatchery scientists take management decisions to control the optimum growth of *Chaetoceros* sp.

Shorter lag phase implies asymmetry in growth profile. So, growth curves with asymmetric growth dynamics (e.g. theta-logistic, Gompertz, extended Gompertz, etc.) should be preferred to model the growth profile of *Chaetoceros* sp. Note that, modelling through rate profile (relative growth rate (RGR), which is the growth rate relative to the initial size of the population) is preferred than the size profile (biomass, abundance, any signature of biomass (OD values, etc.), in capturing the asymmetric growth dynamics[13–15]. In this article, we study the interdependence between initial inocula levels of *Chaetoceros* sp. and the steady state behaviour of its growth profile through the growth curve models, which can theoretically determine different phases (lag, log and stationary, etc.) of the growth curve, based on the relative growth rate.

The organization of rest of the manuscript is as follows. Under materials and methods, the experimental protocol is described with calibration curve of OD and biomass. The model descriptions and experimental data fitting with the identification of growth phases are well illustrated in the same section. Estimation of growth phases under two inocula levels and relative comparisons through statistical analysis are done with proper explanation. Finally, we have an elaborate discussion and provide a conclusion on the overall objectives of the research.

Materials and methods

Experimental design

Chaetoceros sp. used in this experiment was grown in two conical flasks each of volume 1 litre and filled up with 1 litre F/2 medium[16]. These two conical flasks were used for two separate cultures with different inocula levels. *Chaetoceros* inocula were collected from the running stock culture of the lab (AERU Plankton Culture Lab, ISI, Kolkata). Our previous laboratory experiences show that 50 ml initial culture inoculum in 1000 ml culture medium exhibited better culture quality, i.e. the tendency of crashing of the culture is low compared to less than 50 ml inoculum size in 1000 ml culture medium.

In this study, to perform the experiment, two initial inocula were taken – (i) 50 ml and (ii) 50% increment of the first inoculum, i.e. 75 ml initial inoculum to know if there would be any significant difference in the growth profiles of *Chaetoceros*. One of the cultures was started with 50 ml inoculum (0.97×10^6 cells ml^{-1}), denoted as series A and the other culture with 75 ml initial inoculum (1.49×10^6 cells ml^{-1}), denoted as series B for the rest of the manuscript. The series A can be further represented as the PLID, i.e. Population with low initial density and the series B can be represented as the PHID, which stands for population with high initial density. Those initial inocula were taken from the same running culture of *Chaetoceros* sp. (2.01×10^6 cells ml^{-1}; OD value 0.485) and the total experiment was maintained under continuous aeration and illumination (1500 LUX) and constant temperature (23 ± 1°C) in the laboratory. Culture of each inoculum level was maintained in triplicate. Initial cellular density was counted using hemocytometer[12]. First sampling was done at 2–3 min after the primary inoculation and was carried out at every 12 h interval throughout the experimental period for optical density measurement, taken at 688 nm wavelength for visible light[17]. Measuring the optical density of a growing culture is a common method to estimate growth of the species at specific time intervals

because we know that the optical density of a growing culture increases proportionately with the increased concentration of liquid culture[17–19].

For the biomass estimation, at first the samples were centrifuged at 8000 rpm for 10–15 min. Then, the clear supernatant was discarded and the pellet was dried in a desiccator until the weight became constant.

Optical density – the proxy of biomass

Generally, biomass dried weight and cell count are used for depicting the growth profile of any microorganism. Note that, the biomass and the cell count are measured either by using hemocytometer or by assessing the dry cell weight of the species. Both the methods are manually operated and are subject to human experimental error. Recently, an alternative measurement, the optical density (OD) was used to assess the growth profile of the microalgae species by several studies[17,20,21]. Note that, this OD reading is a direct output of the spectrophotometer apparatus; hence less affected by human subjective error. However, it is still debatable weather OD values can be used as a direct signature of the species biomass. An existing study[21] for other species, also observed that both methods referred above (direct cell counting and biomass dry weight evaluation) in addition to calibration curve with OD, are suitable for cell density evaluation.

In this experiment, we study the growth profile of *Chaetoceros* based on OD values. At the same time, it is imperative to develop a calibration curve of OD and biomass so that we can comfortably use OD as a representor of biomass[21,22]. With respect to developing the calibration curve of OD and biomass of the species, first, we plotted the OD (absorbance at 688 nm wavelength for visible light) on the x-axis and the biomass (dry weight of algal cell mass) on the y-axis for both the series A and B (Figure 1). Then, the relationships between OD and biomass were established by the linear regression model without intercept ($y = mx$), using R software. Following the R^2 values ($R^2 = 0.9935$, $P < 0.001$ for series A; $R^2 = 0.9891$, $P < 0.001$ for series B), we can easily state that there is a linear relationship between OD and biomass of *Chaetoceros* sp. Thus, OD can serve as the proxy of biomass and we can duly use OD as the representative of the biomass for our study.

After completing the experiment, we had two time-series datasets of OD values – series A and series B. Each dataset has 29 time points, which represent 336 h of the total experimental time. The OD value at a certain time point (t) can be used as a replacement of the size variable.

Our next objective was to find a suitable growth curve to represent the nature of the growth profile of the species. We know that the growth profile of any species can be well understood through the standard growth curve model. Note that, it is not easy for the experimenter to identify the proper model from a rich class of growth curve family. Previous studies in this domain suggest that the identification of a suitable model is easier through the RGR profile instead of size profile[14]. Apart from this, a single sigmoidal curve is not sufficient to explain the approximately reverse bathtub type profile curve of the *Chaetoceros* growth (Figure 2 *a* and *d*). However, when we plot time versus RGR profile, the data might have good agreement with the common growth curves. For plotting, we used Fisher's RGR as an empirical estimate of relative growth rate, which is given by $(1/\Delta(t))\ln(X(t_2)/X(t_1))$, where $X(t_2)$ and $X(t_1)$ are the sizes at time point t_2 and t_1 respectively and $\Delta(t) = t_2 - t_1$. For example, Figure 2 *a* and *d* cannot be modelled through the common growth curves as the profiles do not exhibit sigmoidal shapes. If we would like to develop the model for RGR profile (Figure 2 *b* and *e*) it has a close synergy with the Gompertz RGR function. So, the first and most important step for summarizing the growth profiles of the two series (A and B), is to estimate the RGR profile correctly based on the OD values. The growth curve literatures suggest that RGR is either size or time dependent. For an initial guess of the growth curve models which have proximity with respect to experimental data (series A and B), we plotted the RGR profiles against both, time and size (Figure 2 *b*, *e*, *c* and *f* respectively). RGR plots against time and size exhibit a nonlinear trend. This is a clear indication that the data have close resemblance with either power logistic or Gompertz model. After incorporating a brief introductory description (next section) about these models, we fit the experimental data through the nonlinear least square.

The model

Growth models can be broadly classified into two categories: (1) size covariate models and (2) time covariate models based on the form of the RGR function[23]. For size covariate model (logistic, theta logistic, limiting logistic) RGR is an explicit function of size, but RGR of species is a function of age/time for the time covariate case[24]. To understand different models that are used to represent population dynamics, we can start by looking at a general equation for the population growth rate (change in the number of individuals in a population over time)

$$\frac{1}{x(t)}\frac{\mathrm{d}x(t)}{\mathrm{d}t} = R(t) = r. \tag{1}$$

By integrating this equation we get

$$x(t) = x(0)e^{rt}, \tag{2}$$

where $x(t)$ is the population size at time point t, $R(t)$ the RGR at time point t and r is the per capita rate of increase.

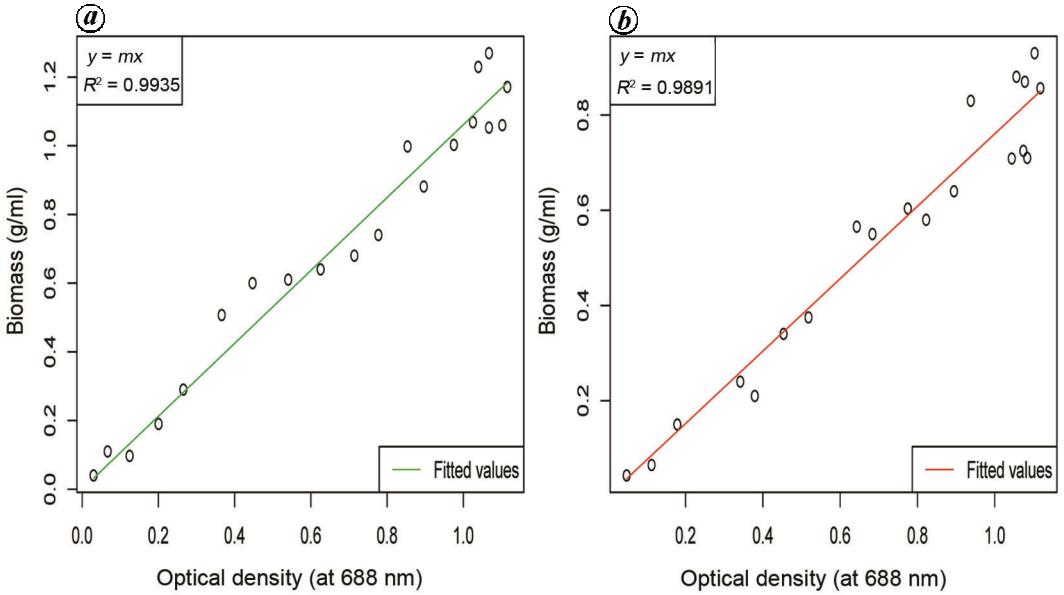

Figure 1. The calibration curve of optical density (OD) and the biomass of *Chaetoceros* sp. where (***a***) represents the linear relationship between the optical density, taken at 688 nm visual light wavelength (plotted on *x*-axis) and the biomass in gm/ml (plotted on *y*-axis) for series A (50 ml initial inoculum size) and (***b***) represents the linear relationship between the optical density, taken at 688 nm visual light wavelength (plotted on *x*-axis) and the biomass in gm/ml (plotted on *y*-axis) for series B (75 ml initial inoculum size). The equations for regression model and the R^2 values are provided in the top left corner in both (***a***) and (***b***). The circles (○) represent the observed values and the green, red lines represent the fitted values for series A and series B respectively.

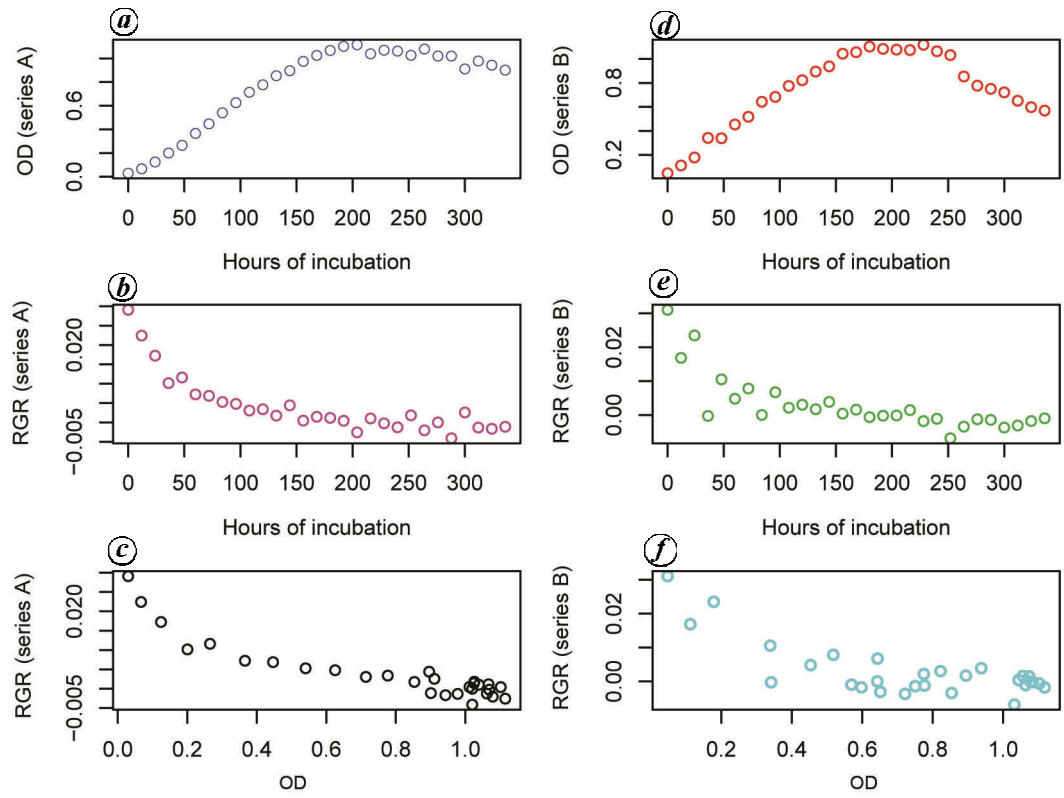

Figure 2. Advantage of the relative growth rate (RGR) modelling over size modelling based on OD values. (***a***), (***d***) exhibit the complete growth profile of *Chaetoceros* sp. during the entire experimental time period (336 h) for series A (50 ml initial inoculum size) and series B (75 ml initial inoculum size) respectively. The incubation time (hours) is plotted on the *x*-axis and the optical density (absorbance at 688 nm wavelength of visible light) is plotted on the *y*-axis accordingly. The RGR profiles against time (hours of incubation) are depicted in (***b***) and (***e***) for the series A and B respectively. Similar plots of RGR profiles against size (OD values) are exhibited in the (***c***) and (***f***) for the series A and B respectively. The presence of the decay phases in the (***a***) and (***d***), violate the assumptions of the sigmoidal growth pattern. But in comparison, the RGR profiles against time (***b*** and ***e***) have a close synergy with the Gompertzian rate pattern.

Let us discuss some of the most common growth curve models from the literature.

Theta-logistic and logistic growth model: Theta-logistic model[25,26] is known as a generalized logistic model in ecological literature[13], where θ is the only parameter that regulates the density of the population. The theta-logistic model is represented by the differential equation

$$\frac{\mathrm{d}x(t)}{\mathrm{d}t} = rx(t)\left(1-\left(\frac{x(t)}{k}\right)^{\theta}\right). \tag{3}$$

By solving this equation we get

$$x(t) = \frac{k}{\left(1+\left(\left(\frac{k}{x(0)}\right)^{\theta}-1\right)\mathrm{e}^{-\theta rt}\right)^{1/\theta}}, \tag{4}$$

where r is the per capita rate of increase, k the carrying capacity and θ is the curvature parameter. The model 3 reduces to logistic model when $\theta = 1$, with the solution

$$x(t) = \frac{k}{(1\ +\ b\mathrm{e}^{-rt})}. \tag{5}$$

Gompertz curve: a limiting theta-logistic model: The most popular member of time covariate family is the Gompertz model which describes the dynamics of a population that grows with an intrinsic rate of growth that decays exponentially. The relative growth rate of this model can be defined as

$$\frac{1}{x(t)}\frac{\mathrm{d}x(t)}{\mathrm{d}t} = b\mathrm{e}^{-at}. \tag{6}$$

By integrating the eq. (6) we get

$$x(t) = x_0 e^{((b/a)(1-\exp(-at)))}, \tag{7}$$

where a and b are real positive constants.

We consider eq. (3) as a limiting form of the model where $\lim_{\theta\to 0}$. Ignoring the higher order terms in θ and taking the limit as $\theta \to 0$ the model 3 approaches

$$R(t) = \frac{1}{x(t)}\frac{\mathrm{d}x(t)}{\mathrm{d}t} = r\theta\ln k\left(1-\frac{\ln\ x(t)}{\ln k}\right). \tag{8}$$

Hence, for a well defined model in the limit, r must tend to infinity so that $r\theta \ln k$ approaches a finite constant, say ϕ in the limiting model and gives

$$\frac{1}{x(t)}\frac{\mathrm{d}x(t)}{\mathrm{d}t} = \phi\left(1-\frac{\ln\ x(t)}{\ln k}\right)$$

$$\Rightarrow \frac{\mathrm{d}x(t)}{\mathrm{d}t} = x(t)\phi\left(1-\frac{\ln\ x(t)}{\ln k}\right).$$

Integrating the eq. (8), we get the solution of $x(t)$ as

$$x(t) = k\mathrm{e}^{\ln(x(0)/k)\exp(-\phi t)}. \tag{9}$$

The eq. (9) is just like a size covariate transformed format of the Gompertz growth model.

In growth curve study, usually the lag, log and stationary phases can be characterized by a single symmetric/asymmetric growth equation. It is evident from the RGR curve fitting that the population of *Chaetoceros* under study showed very rapid growth at the initial phase. It is well known that the usual growth profile of *Chaetoceros* is composed of four consecutive growth phases, viz. lag, log, stationary and the decay.

In our study, when OD versus RGR was plotted with the experimental data, a concave upward relationship was observed between OD and RGR, which motivates us to fit theta-logistic model in this case. But the OD plot suggests a very short lag phase and a sharp log phase, which indicates that the species must have been very strong r strategists, i.e. having a very high reproduction rate. Note that, when θ is very small, r is very high but $r\theta \ln k$ is moderately large which indicates that the theta logistic family reduces to Gompertz growth equation. In this case, limiting theta-logistic growth profile must be appropriate rather than the classical theta-logistic model[27]. For the time covariate when we plot age (time) versus RGR graph, it exhibits an exponential decay relationship between OD and RGR which has a signature of Gompertz Growth Law. So, limiting theta logistic or Gompertz may be a good candidate to model the growth phenomena of *Chaetoceros*.

Growth curve fitting

The objective of curve fitting is to describe the experimental data with the help of a model (function or equation) and to estimate the parameters associated with this model. In our experimental data, it is clear that the response variable is not linearly related to other variables. So, we fit this data, based on nonlinear least squares method (nls) and the model parameters are estimated using nonlinear regression routine implemented in statistical software R. To identify the best-fitted model, we have used Akaike Information Criterion (AIC)[28] which is a measure that estimates the quality of each model, relative to each of the other models. If k is the number of estimated parameters in the model and $\hat{L}$ is the maximum value of the likelihood function for the model, then the

Table 1. Estimation of parameter values using logistic model

Model	$\hat{r}$	*P* value	$\hat{k}$	*P* value	AIC	RMSE
Logistic (series A)	0.019	0.000	0.984	0.000	–245.418	0.003
Logistic (series B)	0.017	0.000	0.895	0.000	–213.128	0.005

The estimated values of the model parameters ($\hat{r}$ and $\hat{k}$) are provided in this table, where, $\hat{r}$ = estimated value of the growth rate and $\hat{k}$ = estimated value of the carrying capacity. The *P* values suggest that the parameter values are significant (*P* values ≅ 0). The performance of the model can be described by the AIC and RMSE values.

Table 2. Estimation of parameter values using Gompertz model

Model	$\hat{a}$	*P* value	$\hat{b}$	*P* value	AIC	RMSE
Gompertz (series A)	0.028	0.000	0.020	0.000	–285.034	0.001
Gompertz(series B)	0.029	0.000	0.027	0.000	–237.583	0.003

The estimated values of the model parameters ($\hat{a}$ and $\hat{b}$) are tabulated here. The *P* values suggest that the parameter values are significant (*P* values ≅ 0). The performance of the model can be described by the AIC and RMSE values.

Table 3. Estimation of parameter values using Gompertz size model

Model	$\hat{a}$	*P* value	$\hat{b}$	*P* value	$\hat{c}$	*P* value	AIC	RMSE
Gompertz size (series A)	1.175	0.000	1.498	0.000	0.221	0.000	–83.677	0.026
Gompertz size (series B)	1.184	0.000	1.247	0.000	0.212	0.000	–76,922	0.031

The estimated values of the model parameters ($\hat{a}, \hat{b}$ and $\hat{c}$) are tabulated here. The *P* values suggest that the parameter values are significant (*P* values ≅ 0). The performance of the model can be described by the AIC and RMSE values.

AIC value of the model can be estimated from $2k - 2\ln \hat{L}$. The model having the lowest AIC value represents the best-fitted model for a given dataset. Additionally, in order to choose the final best-fitted model among all the best-fitted models, the differences of the AICs are calculated[29]. Let, $\Delta_i = \text{AIC}_i - \text{AIC}_{\text{mean}}$, where AIC_i is the AIC of the *i*th model and AIC_{mean} is the lowest among the all AICs of the models under consideration. To choose the best model, we may follow the following rule.

(1) If, $\Delta_i < 2$, then there is sufficient support to choose *i*th model.
(2) If, $2 < \Delta_i < 4$, then the *i*th model has strong support to be accepted.
(3) If, $4 < \Delta_i < 7$, then the *i*th model does not have considerable support to be accepted.
(4) Finally, the models with $\Delta_i > 10$ should not be accepted.

Another frequently used measure for selection of the best model for the observed data is residual mean square error (RMSE) which measures the differences between predicted values by a model or an estimator and the values actually observed[30,31]. Like AIC, the lowest RMSE value of a model is also considered as the measure for identification of the best fitted model[32]. The estimated values of the parameters, AIC and RMSE values are summarized in Tables 1 and 2).

By observing the p-values and RMSE values of the model parameters in Tables 1 and 2, we can identify that the estimated values of the parameters of logistic RGR model and Gompertz model are significant for both the series A and B. Observed and estimated values of RGR of logistic model and Gompertz model for both the data series are represented in Figures 3 and 4 respectively. AIC and RMSE values for two RGR models are given in Tables 1 and 2). When we compare the AIC and RMSE values for both logistic and Gompertz models, we observe that the Gompertz RGR model has lower AIC and RMSE values than the logistic RGR model. In addition, the Δ values (as given previously) of logistic model compared to the Gompetz RGR model are found to be 39.616 and 24.455 for series A and B respectively. In both cases, Δ values are greater than 10. Hence, Gompertz RGR provides better fit.

Again, the parameter values are estimated using the Gompertz size model. The estimated values of the parameters, AIC and RMSE values are summarized in the Table 3.

According to Table 3, all the parameter values of the Gompertz size model are significant (observed and estimated values of the Gompertz size model for both the data series are represented in Figure 5). However, both the AIC and RMSE values of the Gompertz RGR model (Table 2) are less than the Gompertz size model (Table 3). Again it should be noted that the Δ values as in the previous case, for series A and B of the Gompertz size model compared to Gompertz RGR model, are found to be 201.357 and 160.661, which are significantly >10. Hence, Gompertz size model should not be accepted compared to Gompertz RGR model. This indicates that modelling through RGR is better than modelling based on size.

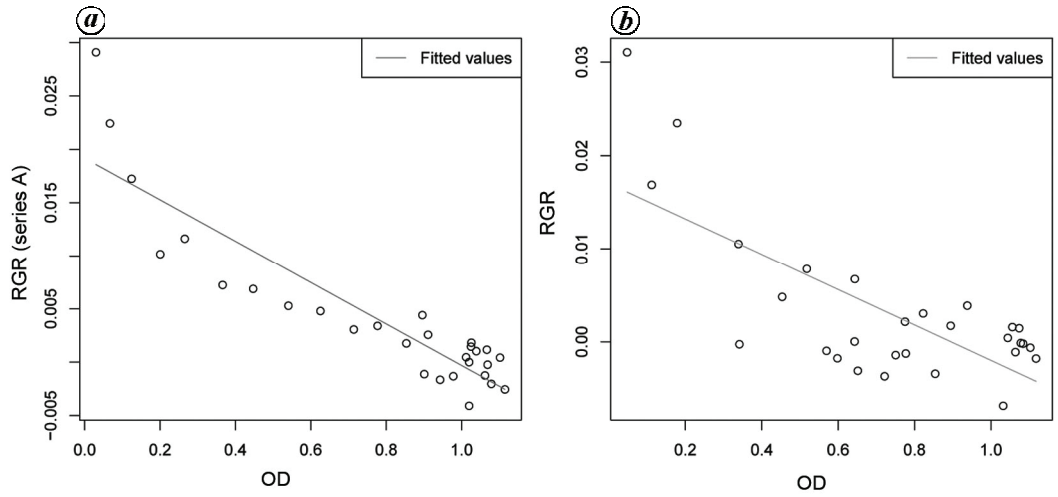

Figure 3. Logistic RGR fitting based on observed values of series A and B (see (***a***) and (***b***) panels) respectively. The OD (size) values are plotted on the *x*-axis and the RGR of OD values are plotted on the *y*-axis. The circles (○) represent the observed values and the pink, green lines represent the fitted curves for the series A and B respectively.

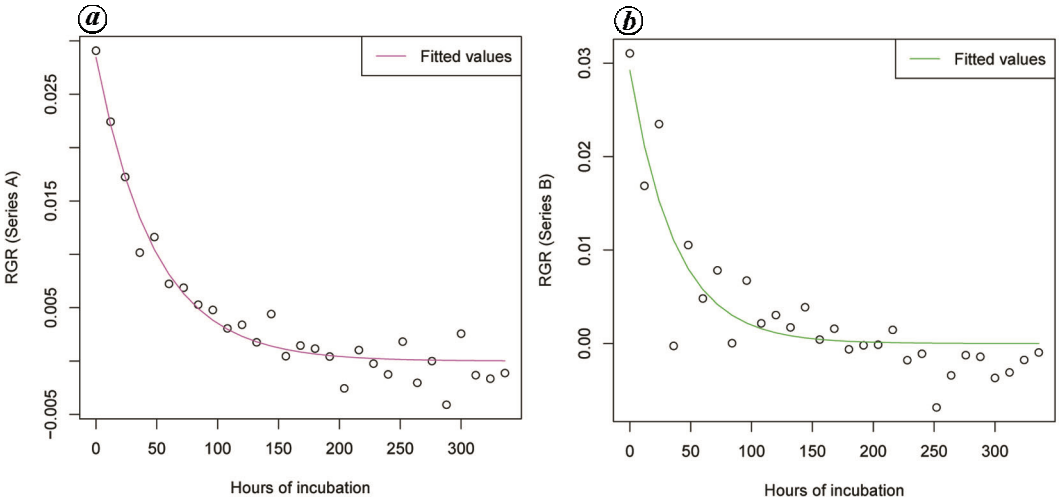

Figure 4. Gompertz RGR fitting based on the observed values of series A and B (see (***a***) and (***b***) panels) respectively. The time points (incubation hours) are plotted on the *x*-axis and the RGR of OD values are plotted on the *y*-axis. The circles (○) represent the observed values and the pink, green lines represent the fitted curves for the series A and B respectively.

Different phases of the growth curve

In the present study, when population size is plotted against time, a sigmoidal curve is achieved (Figure 6). In general, any sigmoidal growth curve can be divided into three major phases of growth, viz. an initial phase or lag phase, an exponential phase or log phase and lastly a stationary phase.

The length of the lag phase and the strength of the log phase can be determined theoretically and estimated by the help of the model of Zwietering *et al.*[33]. According to this model, a sigmoidal curve can be approximated by three straight lines: AB, BC and CD (Figure 7). The point of inflection is achieved at point H on the curve, where the specific growth rate is maximum. Now, if a tangent is drawn through the point of inflection and extended up to the *x*-axis, then this tangent would cut the *x*-axis at the point *E*. Let, the quadrate of this point *E* be (λ, 0). Then the length of λ would be the estimator of the lag phase of the sigmoidal asymmetric growth curve. Moreover, if the angle at the point of inflection is μ_m then it would be the estimator of the log phase. Being the slope of the curve, μ_m regulates the log phase of the growth curve. After the log phase, a final phase is reached when the rate decreases and finally arrives at zero, the steady state. We can precisely define the time span of the lag, log and stationary phases of the growth curve in the following way. The intervals [0, t_1) and [t_1, t_2) can be represented as the span of lag and log phases respectively. The interval [t_2, ∞) corresponds to the stationary phase of the growth curve (Figure 7). The growth curve may show a decline after attaining the steady state. This kind of behaviour

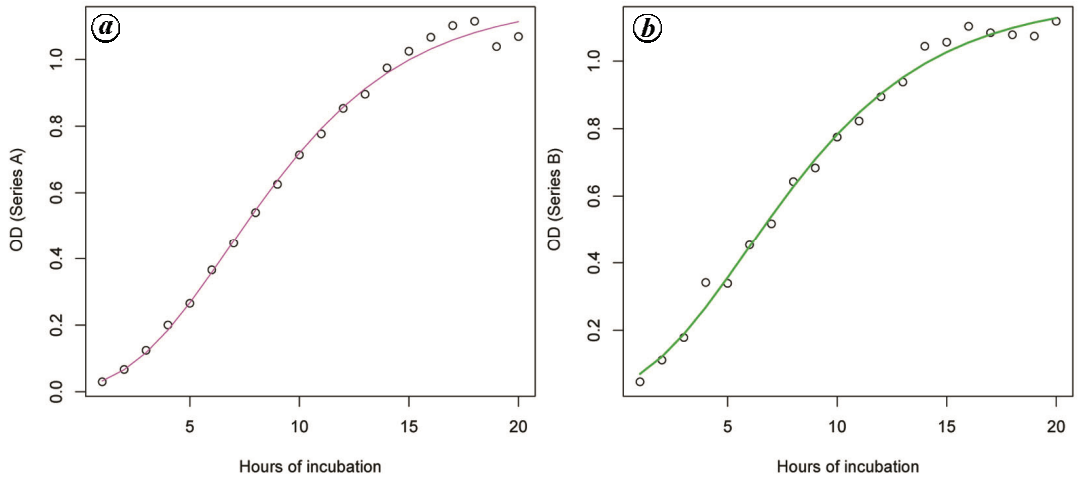

Figure 5. Fitting of Gompertz growth curve models, using OD values up to the stationary phases for the series A and B respectively (see panels (***a***) and (***b***)). The time points (incubation hours) are plotted on the *x*-axis and the OD values are plotted on the *y*-axis. The circles (o) represent the observed values up to the stationary phases and the pink, green lines represent the fitted Gompertz curves.

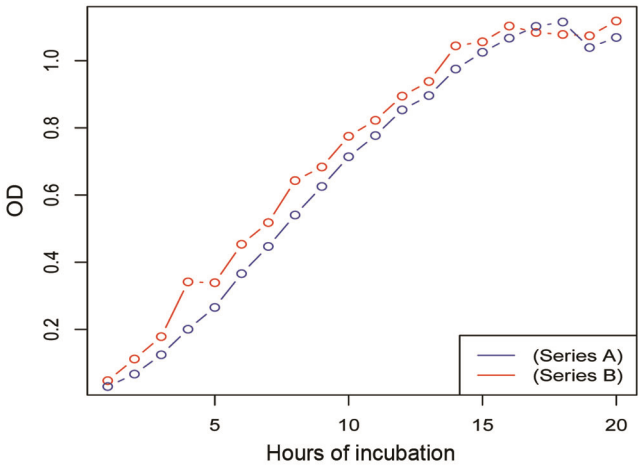

Figure 6. Comparison of the size profiles based on the OD values of the series A and B respectively. The blue and red circles with lines, represent the series A and B respectively.

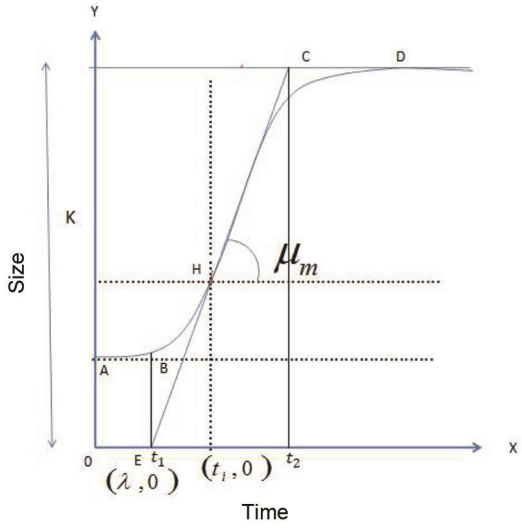

Figure 7. The graphical representation of the three growth phases (lag, log and stationary) of any general sigmoidal growth curve. The lag and log phases are estimated by the parameters λ and μ_m respectively. Precisely, the time span of the lag, log and stationary phases of the growth curve can be described as follows. The intervals $[0, t_1)$ and $[t_1, t_2)$ can be represented as the span of lag and log phases respectively. The interval $[t_2, \infty)$ corresponds to the stationary phase of the growth curve.

is called the decay phase and is not considered here for modelling.

Results

Determination of different phases of growth profile

Determination and estimation of λ and μ_m for both series A and B are done following the technique of Zwietering *et al.*[33]. The determination procedure is summerized below.

Equation (9) can be written like Gompertz equation, i.e.

$$x(t) = ke - \exp\left[\ln\frac{x(0)}{k} - \phi t\right], \tag{10}$$

$$x(t) = ae - \exp[b - ct], \tag{11}$$

where $\ln(x(0)/k) = b$, $k = a$ and $\phi = c$.

At the inflection point where $t = t_i$, the second derivative is equal to zero. Then we calculate

$$\frac{\mathrm{d}^2x(t)}{\mathrm{d}t^2} = 0 \rightarrow t_i = b/c, \tag{12}$$

now, we get the first derivative at the inflection point t_i

$$\frac{dx(t)}{dt} = ace - \exp(b - ct)\exp(b - ct). \quad (13)$$

From eq. (13) we get $\mu_m = (dx(t)/dt) = ac/e$,

Substituting the value of t_i in eq. (10) we get Y_1

$$Y_1 = k\exp\left(\ln\frac{x(0)}{k}\exp - \phi\frac{b}{c}\right). \quad (14)$$

The description of tangent line through the inflection point is

$$Y = \mu_m t + Y_1 - \mu_m t_i. \quad (15)$$

The lag time is defined as the t-axis intercept of the tangent through the inflection point,

$$\mu_m\lambda + Y_1 - \mu_m t_i = 0. \quad (16)$$

The theoretical value of λ is

$$\lambda = \frac{b-1}{c}. \quad (17)$$

Previously we had estimated the parameter values of Gompertz model by nonlinear least square method. Using this parameter value we also estimated the values of lag phase, log phase and the point of inflection of *Chaetoceros* sp. The estimated values are summarized in Table 4.

Testing of hypotheses

From our experimental data, we estimate the time points where the λ values exist both for series A and B say, λ_A and λ_B. We can test the time points at which the λ value observed are same or different along two data series. So, our null hypothesis is

$$H_0 : \lambda_A = \lambda_B, \quad (18)$$

against the obvious alternative

$$H_1 : \lambda_A > \lambda_B,$$

Table 4. Estimated values of different phases of growth profile of *Chaetoceros* sp.

Data	lag phase (λ)	log phase (μ)	Point of inflection (t_i)
Series A	2.253	0.095	6.878
Series B	1.163	0.092	5.860

Estimated values for the different phases and inflection points for both the experimental set up of the growth profile of *Chaetoceros* sp. are provided in this table. From this table, we can compare between the two experimental set-up by observing these estimated values.

From the asymptotic properties of MLE we have, $\hat{\theta}_i \sim N(\theta_i, \mathrm{Var}(\hat{\theta})_i))$, for $i = 1, 2, 3$ and $\hat{\lambda}_k \sim N(\lambda_k, \mathrm{Var}(\hat{\lambda}_k)$, for $k = A, B$ where $\hat{\theta}_i = (\hat{\theta}_1, \hat{\theta}_2, \hat{\theta}_3) = (\hat{a}, \hat{b}, \hat{c})$. By the invariance property of maximum likelihood estimator, λ_A and λ_B are functions of the parameters b, c. So the MLE of λ_A and λ_B are $\hat{\lambda}_A$ and $\hat{\lambda}_B$ respectively, where $\hat{\lambda}_A = (\hat{b} - 1)/c$. The variance of the above estimators is the asymptotic variance. The test statistic of this test is given by

$$\tau_1 = \frac{(\hat{\lambda}_A - \hat{\lambda}_B) - (\lambda_A - \lambda_B)}{\sqrt{\mathrm{Var}(\hat{\lambda}_A) + \mathrm{Var}(\hat{\lambda}_B)}}. \quad (19)$$

To test the equality of log phases between two series of data, we consider the following hypothesis given by

$$H_0 : \mu_{mA} = \mu_{mB}, \quad (20)$$

against the obvious alternative,

$$H_1: \text{not } H_0,$$

and the test statistic is

$$\tau_2 = \frac{(\hat{\mu}_{mA} - \hat{\mu}_{mB}) - (\mu_{mA} - \mu_{mB})}{\sqrt{\mathrm{Var}(\hat{\mu}_{mA}) + \mathrm{Var}(\hat{\mu}_{mB})}}. \quad (21)$$

The null distribution of both the test statistics τ_1 and τ_2 is $N(0, 1)$. So the null hypotheses are rejected at α level of significance if $\tau_1 > z_\alpha$ and $|\tau_2| > z_{\alpha/2}$ respectively, where z_α is the upper $100(1 - \alpha)$ percentile of the standard normal distribution. To evaluate the test statistics, τ_1 and τ_2, we need to calculate the variance of $\hat{\lambda}_A$ and $\hat{\mu}_{mA}$. The variance is calculated from the following formula involving the function of estimators.

$$\mathrm{Var}[\phi(\hat{a}, \hat{c})] = \mathrm{Var}(\hat{a})\left(\frac{\partial\phi}{\partial a}\right)^2\Bigg|_{\hat{a},\hat{c}} + \mathrm{Var}(\hat{c})\left(\frac{\partial a}{\partial\phi}\right)^2\Bigg|_{\hat{a},\hat{c}}$$

$$+2\mathrm{Cov}(\hat{a}, \hat{c})\left(\frac{\partial\phi}{\partial a}\right)\Bigg|_{\hat{a},\hat{c}}\left(\frac{\partial a}{\partial\phi}\right)^2\Bigg|_{\hat{a},\hat{c}}, \quad (22)$$

where $\phi(\hat{a}, \hat{c})$ is a nonlinear function of a and c (ref. 34).

Based on this testing of hypotheses it is found that there is a significant difference between the lag phases of two data series (P value 0.009) and the test statistic value is 2.357. Thus, the null hypothesis (eq. (18)) is rejected at 5% level of significance. In case of log phases the observed value of the test statistic is 0.344 and P value is 0.365. Therefore, the null hypothesis (eq. 20) is accepted at 5% level of significance. It signifies that there is no significant difference between the log phases of the two data series.

Discussions and conclusion

In microalgae culture, key complexities are coupled with production processes and related high operational costs. Difficulties are involved in the overall maintenance of a reliable culture for commercial purposes. Note that, these high expenditures make almost half of the economic cost of a fish culture plant[35]. To reduce the production costs and fulfil the demand of the hatchery industries, an optimum culture condition of microalgae is required. So, research on optimum culture technique of microalgae by monitoring and controlling growth profiles is an important study area to be explored. Although the study of the nature of the growth profile is an essential step in the microalgae technology, its detailed study has been largely ignored[36]. Analysis of the observed data sets by using conceptual models can be a new approach and an alternative tool in the optimization process of microalgae culture for commercial usages.

In the present study, we have studied the nature of the growth profiles of a commercially valuable algal species, *Chaetoceros* sp. under two different experimental conditions. In microalgae culture, initial inoculum has immense effect on the biomass yield[37], a key indicator of the growth profile. To identify this effect, we have conducted the growth experiment of *Chaetoceros* sp. in laboratory condition under two levels of inoculum in *F*/2 medium. We obtained the data in terms of OD values for the two levels of inocula. We assumed OD values as a signature of the biomass. To support this assumption, we developed a calibration curve of OD and biomass and observed that there exists a strong linear relationship between OD and biomass for both the levels of inocula of *Chaetoceros* sp. We chose the best fitted model (Gompertz model) using RGR profiles of OD values for identification of critical change points of different growth phases to understand the variations in growth trajectories accurately. It is noteworthy, that small discrepancies in the span of the different phases of growth are generally overlooked in simple growth curve observation method. It is well known that the spans of lag and log phases (first two phases of a growth curve) are the key factors by which we can compare the maturity time of the species for the two levels of inocula. The shorter lag phase and rapid log phase may encourage earlier maturity for the species. We determine the estimates of lag and log phases by using the parameter estimates of the fitted model.

The three phases of the growth curve model can be described by three parameters. The parameter μ_m is defined as the slope of the tangent in the inflection point. This parameter can also be interpreted as the magnitude of the maximum specific growth rate, which is achieved at the point of inflection. The slope of the tangent can be used as an indicator of log phase. The parameter λ is defined as the x-axis intercept of this tangent. This can be used as a proxy of the lag phase.

These phases can be well understood from Figure 7. The growth curve has the asymptote at $x(t) = k$. The tangent EC at the point of inflection H, intercepts the asymptote at the point C. The segment OE, which is the x-axis intercept of the tangent EC at the point of inflection, is representative of the lag phase. Note that, the slope of the tangent EC is an indicator of the log phase. The length CD can be interpreted as the proxy of the stationary phase.

The hypothesis of the equality of the expected lag phases of the two growth profiles, which is generated from the data with two initial inoculum sizes is rejected with reasonably low P values (0.009).

In comparison with the hypothesis of the equality of the expected log phases of the two growth profiles was accepted with reasonably high P values (0.365). This implies that the magnitude of the maximum specific growth rate at the point of inflection is almost the same for both the populations. But surprisingly, the population B reaches the point of inflection 12 h earlier than population A (Table 4).

It is interesting to note that, the magnitude of the maximum specific growth rate for both the series is the same. Naturally, the series A, PHID should reach its maximum value earlier compared to series B, PLID. Growth rate of the dense population is reduced gradually after attaining maximum specific growth. Note that, the PLID reaches its maximum specific growth 12 h later. In the meantime, the PHID loses its growth rate in significant amount. The growth rate of the PLID also starts decreasing after it attains maximum specific growth rate. As a result, two growth trajectories ultimately merge together when they approximately attain steady state. It happens after 180 h of incubation. Note that, the amount of nutrients for both the samples PHID and PLID are the same in the experiment performed in the conical flasks with exactly the same volume. An individual for both the samples PHID and PLID needs the same amount of nutrients per unit time for supporting natural growth. Moreover, an individual also needs an additional proportion of nutrient to compensate the loss of energy due to competition. Naturally, an individual has to utilize more nutrients for this compensation in PHID sample, compared to PLID. So, the possibility of unutilized nutrient is more for series A instead of series B, when the species achieves its steady state. Here, the relationship between the abundance of individuals and the competitions under fixed nutrient condition is identified specifically with the help of modelling approach. So, modelling of growth trajectories under different competition levels can be a good alternative for understanding these types of complex relationships.

We observe a decline in the growth profile after the steady state continues up to 120 and 70 h for series A and series B respectively. Note that, series B shows a rapid decay compared to series A. The species takes the necessary

food for its survival from the unutilized nutrients in the medium during the stationary phase. In this phase, all the consumed nutrients are utilized only for the daily basic need, but not for the growth rate development. The species can survive with this nutrient backup up to a certain period. Obviously, this period must be less for series B compared to series A, as the unutilized nutrients for series A is more than the series B.

If the series B was not a nutrient-limited condition and there is continuous supply of fresh nutrients (like, continuous culture)[6], then it may reach steady state earlier than series A. However, the experiment needs more cost for this additional nutrient. On the other hand, if the experimenter runs a cost-effective experiment in terms of the nutrient, he/she has to wait significant hours for completion of the experiment. Note that, in the second case, the running cost of the experiment is higher. Here, the experimenter can apply the theoretical model to tune the maintenance parameters (time of supply of nutrients, oxygen, light, etc.) of the culture by identifying the transition point of different phases of growth. So, there must be a trade-off from the experimenter; he/she can arrange more nutrients for the early development of the end product or wait patiently for an additional period for the end product. Thus, our modelling approach allows experimental scientists of the hatchery industries take management decisions through this trade-off. Moreover, our modelling approach may also be advantageous over using sophisticated instruments, in terms of expenses and identification of the transition point and duration of the growth phases accurately.

Thus, the theoretical (modelling) approach considered in this article, seems to be effective practically in standardizing the optimal culture condition, monitoring, analysis of growth profiles and understanding complex relationships of microalgae. In addition, modelling of experimental data can help hatchery scientists take proper management decisions to produce a cost-effective culture protocol for commercial usage.

1. Brown, M. R., Nutritional value and use of microalgae in aquaculture. Avances en Nutricion Acucola VI. Memorias del VI Simposium Internacional de Nutricion Acucola. 2002, **3**, 281–292.
2. Simon, C. M., The culture of the diatom *Chaetoceros gracilis* and its use as a food for penaeid protozoeal larvae. *Aquaculture*, 1978, **14**(2), 105–113.
3. Napolitano, G. E., Ackman, R. G. and Ratnayake, W. M. N., Fatty acid composition of three cultured algal species *Isochrysis galbana*, *Chaetoceros gracilis* and *Chaetoceros calcitrans* used as food for bivalve larvae. *J. World Aquacult. Soc.*, 1990, **21**, 122–130.
4. Creswell, L., Phytoplankton culture for aquaculture feed. Southern Regional Aquaculture Center, SRAC Publication No. 5004, September 2010.
5. Fabregas, J. and Herrero, C., Marine microalgae as a potential source of minerals in fish diets. *Aquaculture*, 1986, **51**(3–4), 237–243.
6. Perumal, P., Prasath, B. B., Santhanam, P., Ananth, S., Devi, A. S. and Kumar, S. D., Isolation and culture of microalgae. Workshop on Advances in Aquaculture Technology, 2012.
7. Coutteau, P. and Sorgeloos, P., The use of algal substitutes and the requirement for live algae in the hatchery and nursery rearing of bivalve molluscs: an international survey. *J. Shellfish Res.*, 1992, **11**(2), 467–476.
8. Villares, R. and Carballeira, A., Seasonal variation in the concentrations of nutrients in two green macroalgae and nutrient levels in sediments in the Ras Baixas (nw Spain). *Estuar. Coast. Shelf Sci.*, 2003, **58**(4), 887–900.
9. Biswas, H. *et al.*, Response of a natural Phytoplankton community from the Qingdao coast (Yellow Sea, China) to variable CO_2 levels over a short-term incubation experiment. *Curr. Sci.*, 2003, **108**(10), 1901–1909.
10. Collos, Y., Time-lag algal growth dynamics: biological constraints on primary production in aquatic environments. *Mar. Ecol. Prog. Ser.*, 1986, **33**, 193–206.
11. OBrien, W. J., The dynamics of nutrient limitation of phytoplankton algae: a model reconsidered. *Ecology*, 1974, **55**(1), 135–141.
12. Phatarpekar, P., Sreepada, R., Pednekar, C. and Achuthankutty, C., A comparative study on growth performance and biochemical composition of mixed culture of *Isochrysis galbana* and *Chaetoceros calcitrans* with monocultures. *Aquaculture*, 2000, **181**(1), 141–155.
13. Sibly, R. M., Barker, D., Denham, M. C., Hone, J. and Pagel, M., On the regulation of populations of mammals, birds, fish, and insects. *Science*, 2005, **309**(5734), 607–610.
14. Gupta, A., Bhattacharya, S. and Chattyopadhyay, A. K., Exploring new models for population prediction in detecting demographic phase change for sparse census data. *Commun. Stat. Theory Meth.*, 2012, **41**(7), 1171–1193.
15. Mukhopadhyay, S., Hazra, A., Bhowmick, A. R. and Bhattacharya, S., On comparison of relative growth rates under different environmental conditions with application to biological data. *Metron*, 2016, **74**(3), 311–337.
16. Guillard, R. R. and Ryther, J. H., Studies of marine planktonic diatoms: I. cyclotella nana hustedt, and *Detonula confervacea* (cleve) gran. *Can. J. Microbiol.*, 1962, **8**(2), 229–239.
17. Santos-Ballardo, D. U., Rossi, S., Hernandez, V., Gomez, R. V., del Carmen Rendon-Unceta, M., Caro Corrales, J. and Valdez-Ortiz, A., A simple spectrophotometric method for biomass measurement of important microalgae species in aquaculture. *Aquaculture*, 2015, **448**, 87–92.
18. Falkowski, P. and Kiefer, D. A., Chlorophyll a fluorescence in phytoplankton: relationship to photosynthesis and biomass. *J. Plankton Res.*, 1985, **7**(5), 715–731.
19. Goswami, R., Mondal, S., Mandal, S., Padhy, P., Ray, S. and Majumder, S., Effect of temperature and arsenic on *Aeromonas hydrophila* growth, a modelling approach. *Biologia*, 2014, **69**(7), 825–833.
20. Rodrigues, L. H. R., Raya-Rodriguez, M. T. and Fontoura, N. F., Algal density assessed by spectrophotometry: a calibration curve for the unicellular algae *Pseudokirchneriella subcapitata*. *J. Environ. Chem. Ecotoxicol.*, 2011, **3**(8), 225–228.
21. Rocha, J. M., Garcia, J. E. and Henriques, M. H., Growth aspects of the marine microalga *Nannochloropsis gaditana*. *Biomol. Eng.*, 2003, **20**(4), 237–242.
22. Chiu, S. Y., Kao, C. Y., Chen, C. H., Kuan, T. C., Ong, S. C. and Lin, C. S., Reduction of CO_2 by a high-density culture of *Chlorella* sp. in a semicontinuous photobioreactor. *Bioresour. Technol.*, 2008, **99**(9), 3389–3396.
23. Bhattacharya, S., Basu, A. and Bandyopadhyay, S., Goodness-of-fit testing for exponential polynomial growth curves. *Commun. Stat. Theory Meth.*, 2008, **38**(3), 340–363.
24. Gompertz, B., On the nature of the function expressive of the law of human mortality, and on a new mode of determining the value of life contingencies. *Philos. Trans. R. Soc. Lond.*, 1825, **115**, 513–583.

25. Gilpin, M. E. and Ayala, F. J., Global models of growth and competition. *Proc. Natl. Acad. Sci.*, 1973, **70**(12), 3590–3593.
26. Gilpin, M. E. and Case, T. J., Multiple domains of attraction in competition communities. *Nature*, 1976, **261**(5555), 40–42.
27. Saha, B., Bhowmick, A. R., Chattopadhyay, J. and Bhattacharya, S., On the evidence of an allee effect in herring populations and consequences for population survival: a model-based study. *Ecol. Modell.*, 2013, **250**, 72–80.
28. Akaike, H., A new look at the statistical model identification. *IEEE Trans. Automat. Contr.*, 1974, **19**(6), 716–723.
29. Burnham, K. P. and Anderson, D. R., Multimodel Inference: understanding AIC and BIC in model selection. *Sociol. Meth. Res.*, 2004, **33**(2), 261–304.
30. Willmott, C. J., Some comments on the evaluation of model performance. *Bull. Am. Meteorol. Soc.*, 1982, **63**(11), 1309–1313.
31. Tabari, H., Evaluation of reference crop evapotranspiration equations in various climates. *Water Resour. Manage.*, 2010, **24**(10), 2311–2337.
32. Gundogdu, K. S. and Guney, I., Spatial analyses of groundwater levels using universal kriging. *J. Earth Syst. Sci.*, 2007, **116**(1), 49–55.
33. Zwietering, M., Jongenburger, I., Rombouts, F. and Vant Riet, K., Modeling of the bacterial growth curve. *Appl. Environ. Microbiol.*, 1990, **56**(6), 1875–1881.
34. Seber, G. and Wild, C., Nonlinear regression. 2003, 325–365.
35. Guedes, A. C. and Malcata, F. X., Nutritional value and uses of microalgae in aquaculture. InTech, 2012.
36. Havlik, I., Lindner, P., Scheper, T. and Reardon, K., On-line monitoring of large cultivations of microalgae and cyanobacteria. *Trends Biotechnol*., 2013, **31**(7), 406–414.
37. Lu, S., Wang, J., Niu, Y., Yang, J., Zhou, J. and Yuan, Y., Metabolic profiling reveals growth related fame productivity and quality of *Chlorella sorokiniana* with different inoculum sizes. *Biotechnol. Bioeng.*, 2012, **109**(7), 1651–1662.

ACKNOWLEDGEMENTS. We thank the Agricultural and Ecological Research Unit, Indian Statistical Institute, Kolkata for the laboratory facilities and financial support in pursuing the experiment under the ongoing institutional project. We also thank the field assistant, Mr Sandip Chatterjee for his sincere and enthusiastic help in several aspects. We are also grateful to Dr Bapi Saha for providing technical help in submitting the revised manuscript.

Received 14 May 2018; revised accepted 23 August 2018

doi: 10.18520/cs/v115/i12/2275-2286